

DETERMINATION OF LAMINAR FLAME SPEED OF METHANE-AIR FLAMES AT SUBATMOSPHERIC CONDITIONS USING THE CONE METHOD AND CH* EMISSION

DETERMINACIÓN DE LA VELOCIDAD DE DEFLAGRACIÓN LAMINAR DE LLAMAS METANO –AIRE A CONDICIONES SUBATMOSFÉRICAS EMPLEANDO EL MÉTODO DEL CONO Y LA EMISIÓN DE CH*

LUIS FERNANDO LONDOÑO

Grupo Ciencia y Tecnología del Gas y Uso Racional de la Energía, University of Antioquia, luisfer0570@hotmail.com

CARLOS ESTEBAN LÓPEZ

Grupo Ciencia y Tecnología del Gas y Uso Racional de la Energía, University of Antioquia, estebanlopez37@hotmail.com

FRANCISCO CADAVID

Grupo Ciencia y Tecnología del Gas y Uso Racional de la Energía, University of Antioquia, fcadavid@udea.edu.co

HUGO BURBANO

Grupo Ciencia y Tecnología del Gas y Uso Racional de la Energía, University of Antioquia, hurbano@gmail.com

Received for review December 7th, 2011, accepted March 15th, 2013, final version March, 21th, 2013

ABSTRACT: Experimental measurements of laminar flame speed for premixed methane-air flames were carried out for different equivalence ratios at subatmospheric conditions, 852 mbar and 298 K. The flames were obtained using a rectangular port burner with a water cooler system necessary to maintain the temperature of the mixture constant. An ICCD camera was used to capture chemiluminescence emitted by OH-CH radicals present in the flame and thus define the flame front. Laminar flame speed was calculated using the cone method and experimental results were compared with those reported by other authors and the numerical simulations made with the software CHEMKIN using the GRIMECH 3.0 mechanism. In this work it was found that decreasing the barometric pressure from 1013 mbar to 852 mbar generated an increase of 7% in the laminar flame speed.

KEY WORDS: Spectroscopy, CH radicals, ICCD, laminar flame speed, chemiluminescence.

RESUMEN: Mediciones experimentales de la velocidad de deflagración laminar para llamas de premezcla metano-aire fueron realizadas para distintos dosados a condiciones subatmosféricas, 0,852 bar y 298 K. Las llamas fueron obtenidas utilizando un quemador de puerto rectangular el cual cuenta con un sistema de refrigeración por agua, necesario para mantener la temperatura de la premezcla constante. Se utilizó una cámara ICCD para captar la quimioluminiscencia emitida por los radicales presentes en la llama y así definir el frente de llama. La velocidad de deflagración fue calculada empleando el método del cono. Los resultados experimentales fueron comparados con los reportados por otros autores y simulaciones numéricas realizadas con software CHEMKIN empleando el mecanismo GRIMECH 3.0. En este trabajo se encontró que la disminución de la presión atmosférica de 1013 mbar a 852 mbar genera un incremento del 7% en la velocidad de deflagración laminar.

PALABRAS CLAVE: Espectroscopia, radical CH, ICCD, deflagración laminar, quimioluminiscencia.

1. INTRODUCTION

The combustion industry faces new challenges every day in order to increase the efficiency, reliability and flexibility of combustion equipment and also reduce their environmental impact [1]. Besides developing new improved designs and new concepts of burners,

continuous monitoring and optimization of the flames, which are the core of any combustion process, appears as a primary tool to achieve these demands.

Currently, there are limitations in the optimization and permanent control of combustion systems, because monitoring and control techniques are based on the

analysis of exhaust gases. This analysis only allows the determination of the desired air excess and registering the levels of the undesired emissions [1].

Permanent supervision of the flame seems to be the most appropriate alternative for developing safe and efficient strategies for control and optimization of combustion systems.

This work is based on optical methods designed to capture information directly from the flame which can be used to diagnose combustion in a reliable and accurate way. The optical methods used are based on a phenomenon called chemiluminescence.

Chemiluminescence is the emission of light of those molecules that are returning to their ground state after being chemically and thermally excited. In the case of hydrocarbons, the strongest chemiluminescence emission is produced by CH and OH radicals [2].

The chemiluminescence of CH has been used in several research studies as a visualization technique of the flame and has also been proposed in many works as a sensing method in industrial equipment [2]. Chemiluminescence has been used to detect the localization of the flame front, as the radical CH only exists in a thin region of high temperature [2–4].

With optical methods it is possible to achieve a better understanding of some important process combustion parameters. The laminar flame speed is one of these parameters and is important because it contains information about the reactivity, diffusivity and the heat release of the mixture [3]. The flame speed provides important information about how susceptible the flame is to instabilities such as flashback or blowoff [3].

The present work focuses on the determination of laminar flame speed for mixtures of methane and air, varying the equivalence ratio (ϕ) between 0.8 and 1.4 operating the burner at sub-atmospheric conditions, i.e. 852 mbar equivalent to 1500 masl (meters above sea level). Results obtained in this research were compared with those obtained by other researchers at 1013 mbar (0 masl) and also with numerical simulations made in CHEMKINPRO software using the GRIMECH 3.0 reaction mechanism.

2. THEORETICAL BASES

Spectrometry is often used to identify species or substances through the spectrum absorbed or emitted by them. In the case of combustion, spectroscopy is used to detect the emission of excited radicals generated in the reaction zone. The excited radicals return to their ground state after losing excess energy either in the form of electromagnetic waves at a given wavelength or by intermolecular collisions. During hydrocarbon combustion, particularly methane, some of the most common radicals used to study the flame front of a premixed flame are CH, OH and C_2 .

It is important to clarify that emission of excited radicals produced in flames, is a type of chemiluminescence, because the excitement was produced by a chemical process [5].

Table 1 lists the formation reactions of the radical CH*, with their emission bands [1].

Table 1. Formation routes of excited CH* radical and characteristic wavelengths [1].

Radical	Reaction	Wavelength (nm)
CH*	$C_2H + O \rightarrow CO + CH^*$	387.1,
	$C_2H + O_2 \rightarrow CO_2 + CH^*$	431.4

Each one of the radicals emits its energy simultaneously at different wavelengths but there are wavelengths at which this emission is a maximum. The peak intensity emission for the CH radical it is close to 430 nm.

Radiation intensity at a certain wavelength associated with specific excited radicals has been used as an indicator of flame location or heat release rate [1].

Because chemiluminescence emission intensity of radicals is very low, it is necessary to use intensified capture systems. In this experiment an ICCD (*Intensified Charge Coupled Device*) camera was used, with reference PI-MAX 1K RB FG4, which consist of a high resolution CCD sensor coupled with optical fiber, to a second generation intensifier. The CCD sensor resolution is 1024X1024 pixels.

The intensification system has three main components, which are the photocathode, the microchannel plate

(MCP) and the screen phosphate.

In the photocathode, due to the photoelectric effect, photons incident from the light source are converted into electrons, these are driven to the MCP which is a group of thousands of tiny parallel tubes that each contain an electron emitter in their inner walls.

Figure 1 shows the MCP where electrons generated by the photocathode are driven through the channels by a constant field from a voltage (600-900V) applied to the MCP. A portion of the electrons that pass through the channels strike the walls, causing the formation of thousands of electrons. As the collisions continue, the generated electrons hit a phosphorescent screen, emitting light with an intensity that is greater than the initial [6].

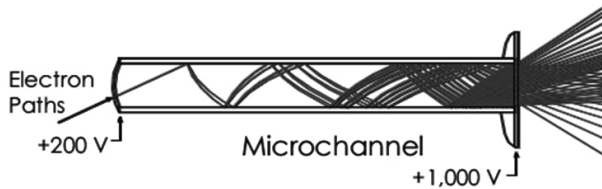


Figure 1. Schematic representation of a MCP [6].

3. METHODOLOGY

3.1. Experimental setup

Flame front images are obtained using an ICCD camera, with a colored filter centered at 430 nm and with a narrow wavelength of 10 nm which allows the passage of the CH emission and blocks radiation outside this wavelength. A typical image is presented in Figure 2, where part (a) is a fully premixed flame and part (b) corresponds to a partially premixed flame which has a diffusion flame front.

The assembly used is shown in Figure 3 where the air flow measurement is made using a calibrated rotameter which operates at 1 bar, with a range of 1.00 to 23.80 standard liters per minute (slpm) and a measurement error of 0.2 slpm. The fuel flow measurement is also done with a calibrated rotameter that operates at 1.00 bar with a measurement range from 0.10 to 4.00 slpm and a measurement error of 0.03 slpm. Given the measurement errors that are recorded with the rotameters the error in the equivalence ratio is $\pm 0.4\%$.

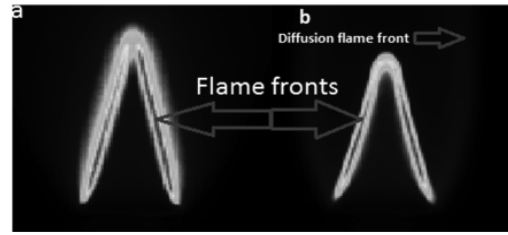


Figure 2. Laminar flame profile. (a) is for $\phi=1$ and (b) is for $\phi=1.4$.

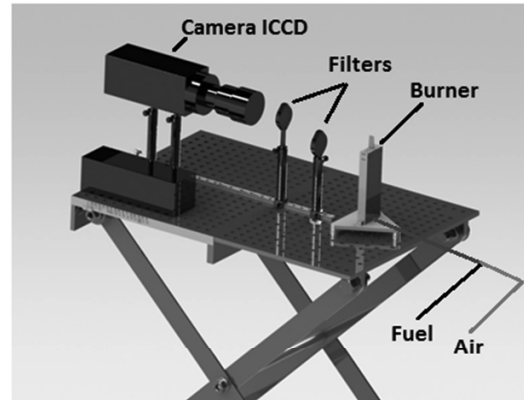


Figure 3. Schematic representation of the experimental assembly.

Laminar flame speeds were calculated from photographs taken with the ICCD camera using the cone method, which consists in determining laminar flame speed (S_L) from the knowledge of the premixture velocity (U) and the angle of the flame front with respect to the vertical (θ) (Ec. 1). The premixture flow rate was controlled to maintain a discharge velocity between 3 and 4.5 times the value of laminar flame speed calculated from numerical simulations [7].

The location and boundaries of the flame front are defined by the maximum change in the intensity registered by the ICCD sensor [8]. Figure 4 shows that the component of the premixture velocity, normal to flame front, is identical to the laminar flame speed (S_L). Therefore, from Figure 4 Eq. 1 is obtained.

$$S_L = U \sin \theta \quad (1)$$

Measurements of laminar flame speed were carried out using a rectangular port burner 5.0 mm x 13.8 mm.

The Reynolds number (Re) was calculated at the burner output, for each equivalence ratio, and the values of Re were between 525 and 1416 which means that all measurements were performed in the laminar regime.

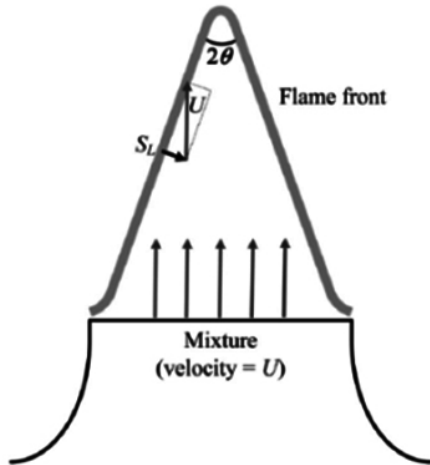


Figure 4. Representation of the flame front.

The burner used guarantees a uniform velocity profile at the burner port. And with this profile, triangular flames with straight edges are obtained. The burner has a water cooling system that is necessary to keep the premix temperature constant, at room temperature (298K).

The digital photos obtained are stored as an array of 1024x1024 pixels. Each one of these pixels records a numerical value according to the magnitude of the intensity captured by the camera. To locate the flame front, the entire array was scanned to determine where the biggest changes in the intensity were.

3.2. Numerical methodology

Numerical calculations of S_L were conducted using the one dimensional premixed flame code PREMIX of the CHEMKINPRO package. Present simulations used the GRIMECH 3.0 reaction mechanism with two barometric pressures: 852 and 1013 mbar. For an accurate prediction of S_L , the recommendations of Bongers and De Goeij [14] were followed; transport properties were evaluated using the multi component diffusion model. Additionally, it has been reported that the accuracy of the calculated S_L is highly sensitive to the number of grid points used in the calculations; using a low number of points can lead to errors from 5 to 10% [15, 16]. Therefore, according to Dlugogorski *et al.* [16], GRAD and CURV values were set lower than 0.01 to generate a grid of more than 1000 points, where S_L values converged and the flame temperature approached the adiabatic flame temperature [7].

4. RESULTS

Flame profiles obtained in the experiment for each equivalence ratio are shown in Figure 5. With values of ϕ lower than 0.8 and higher than 1.4 there was no flame, thus it was only possible to determine S_L for $0.8 < \phi < 1.4$.

Figure 5 shows that for $\phi \leq 1$ a single flame front was obtained, corresponding to a total premixed flame. For $\phi > 1$ there were two flame fronts: the inner flame front corresponding to the premixed flame, and the outer flame front to the diffusion flame. This occurs in partially premixed flames but the laminar flame speed is calculated using the inner flame front of the premixed flame. The maximum value of laminar flame speed is obtained for an equivalence ratio close to 1.08.

Figure 6 shows the experimental results of the present work. These experimental results were compared with the numerical simulation performed at 852 and 1013 mbar and with the experimental results at barometric pressure of 1013 mbar reported by Selles *et al.* [9], Coppens *et al.* [10], Halter *et al.* [11], Bosschaert and Goeij [12]. Comparing the maximum values of laminar flame speed, from Figure 6, there is an increase of 7% when there is a change in barometric pressure from 1013 mbar (0 masl) (38 cm/s) to 852 mbar (1500 masl) (41 cm/s).

The differences in S_L between the results obtained in this work and those reported by other researchers [9-12] are caused by the different barometric pressures. The effect of the pressure on the flame speed can be quantified from equation 2. This expression is obtained by doing mass, chemical species and energy balances applied to the flame front.

$$S_L = \frac{1}{\rho} \left(\frac{\lambda}{c_p} \omega \right)^{1/2} \quad (2)$$

In equation 2, S_L is the laminar flame speed, ρ is the density of the mixture, λ is the thermal conductivity, c_p is the specific heat and ω is the reaction rate. As ρ and ω depend on the barometric pressure, it is expected that the laminar flame speed varies with changes in barometric pressure.

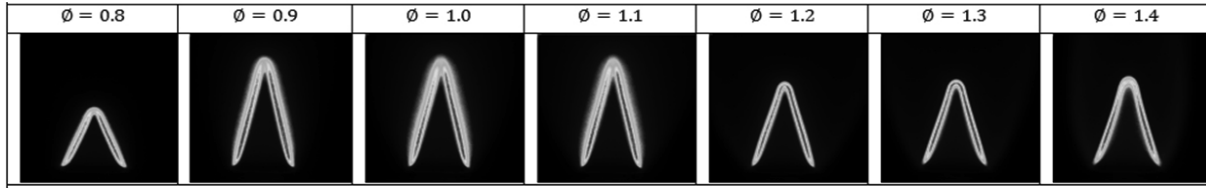


Figure 5. Instantaneous photographs of the flames obtained at different equivalence ratio, using a colored filter centered at 430 nm.

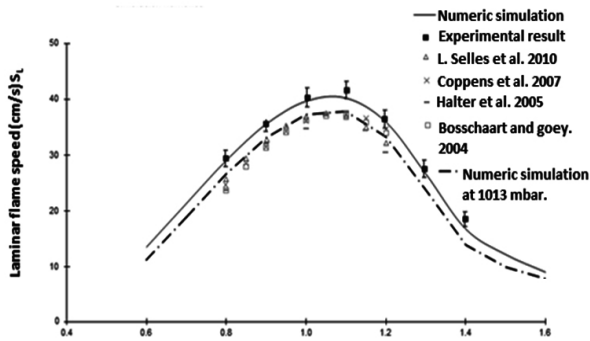


Figure 6. Laminar flame speed Vs. equivalence ratio.

For example, Egolfopoulos and Law [13] suggest an Arrhenius expression (Eq. 3) to determine the laminar flame speed based on the total pressure (p), the overall reaction order (n), the global activation energy (E_a) and the adiabatic flame temperature (T_b):

$$S_L = p^{\left(\frac{n-1}{2}\right)} \exp\left(-\frac{E_a}{2R^0T_b}\right) \quad (3)$$

These authors demonstrated that n decreases as pressure increases, which is directly related to an improvement in termination reactions especially when n is lower than 2, which would be the case in this study.

5. CONCLUSIONS

- The laminarization of premixture allows triangular flames with well-defined straight edges to be obtaining, making accurate measurements of laminar flame speed possible.
- For the experimental conditions (852 mbar) it was only possible to obtain stable flames when $0.8 < \phi < 1.4$. It is well known that for different barometric pressures, there are different ranges of equivalence ratios where is possible to have a stable flame.

- The highest laminar flame speed of a methane-air mixture at 852 mbar barometric pressure, occurs when $\phi \approx 1.08$.
- Varying the barometric pressure from 1013 to 852 mbar generates an increase in laminar flame speed of 7%.
- It was found that the use of ICCD technology is an accurate and valid method to determine the laminar flame speed of a premixed methane-air flame.

ACKNOWLEDGEMENTS

We gratefully acknowledge the financial support provided by Colciencias to develop the project “Desarrollo y evaluación de un quemador de combustión sin llama a gas natural usando aire enriquecido con oxígeno, under contract N° 355-2008” and to the University of Antioquia for the financial support through the Sostenibilidad program for research groups, year 2013/2014.

REFERENCES

- [1] Ballester, J. and Armingol, T.G., Diagnostic techniques for the monitoring and control of practical flames. Progress in Energy and Combustion Science. 36, pp. 375–411, 2010.
- [2] Maurizio, De L., Alexei Saveliev, L. A., Kennedy, S. A. and Zelepouga OH and CH luminescence in opposed flow methane oxy-flames. Combustion & Flame, 149, pp. 435–447, 2007.
- [3] Marques, C.ST. Benvenuti, L.H. and Bertran, C.A., Experimental Study of OH*, CHO*, CH*, and C2* Radicals in C2H2/O2 and C2H2/O2/Air flames in a closed chamber, Combustion Science and Technology, 167, pp. 113–129, 2001.
- [4] Frenillot, J.P., Cabot, G., Cazalens, M., Renou, B. and Boukhalfa, M.A., Impact of H2 addition on flame stability

and pollutant emissions for an atmospheric kerosene/air swirled flame of laboratory scaled gas turbine. *International Journal of Hydrogen Energy*, 34, pp. 3930–3944, 2009.

[5] Pino, F. y Pérez, D., Análisis de elementos-traza por espectrofotometría de absorción molecular ultravioleta-visible. Confederación Española de Cajas de Ahorros, 1^a ed. (10/1983).

[6] Princeton Instruments. Introduction to Image Intensifiers for Scientific Imaging.

[7] Burbano, H.J., Pareja, J. and Amell, A., Laminar burning velocities and flame stability analysis of syngas mixtures at sub-atmospheric pressures. *International Journal of Hydrogen Energy*, 36, pp. 3243–3252, 2011.

[8] Natarajan, J., Nandula, S., Lieuwen, T. and Seitzman, J., Laminar flame speeds of synthetic gas fuel mixtures. Proceedings of GT2005, ASME Turbo Expo 2005: Power for Land, Sea and Air, June 6-9, 2005, Reno-Tahoe, Nevada, USA, GT2005-68917.

[9] Selle, L., Poinot, T. and Ferret, B., Experimental and numerical study of the accuracy of flame-speed measurements for methane/air combustion in a slot burner. *Combustion and Flame*, 158, pp. 146–154, 2010.

[10] Coppens, F. H. V., De Ruyck, J. and Konnov, A. A., Effects of hydrogen enrichment on adiabatic burning velocity and NO formation in methane + air flames, *Experimental Thermal and Fluid Science*, 31, pp. 437–444, 2007.

[11] Halter, F., Chauveau, C., Djebaili-Chaumeix, N. and Gökalp, I., Characterization of the effects of pressure and hydrogen concentration on laminar burning velocities of methane–hydrogen–air mixtures. *Proceedings of the Combustion Institute*, 30, pp. 201–208, 2005.

[12] Bosschaart, K. J. and De Goey, L. P. H., The laminar burning velocity of flames propagating in mixtures of hydrocarbons and air measured with the heat flux method. *Combustion and Flame*, 136, pp. 261–269, 2004.

[13] Egolfopoulos, F. N. and Law, C. K., Chain mechanisms in the overall reaction orders in laminar flame propagation. *Combustion and Flame*, 80, pp. 7–16, 1990.

[14] Bongers, H. and De Goey, L. P. H., The effect of simplified transport modeling on the burning velocity of laminar premixed flames. *Combustion Science and Technology* 175, pp.1915-1928, 2003.

[15] Dong, Y, Vagelopoulos, C. M, Spedding, G. R. and Egolfopoulos, F. N., Measurement of laminar flame speeds through digital particle image velocimetry: mixtures of methane and ethane with hydrogen, oxygen, nitrogen, and helium. *Proceedings of the Combustion Institute*. 29, pp. 1419-1426, 2002.

[16] Dlugogorski, B. Z., Hichens, R. K., Kennedy, E. M. and Bozzelli, J. W., Propagation of laminar flames in wet premixed natural gas-air mixtures. *Transaction of Institution of Chemical Engineers*, 76(B2), pp. 81 – 89, 1998.